HHS Public Access

Author manuscript

DNA Repair (Amst). Author manuscript; available in PMC 2019 June 21.

Published in final edited form as:

DNA Repair (Amst). 2019 January ; 73: 49–54. doi:10.1016/j.dnarep.2018.11.001.

Processing of N^5-substituted formamidopyrimidine DNA adducts by DNA glycosylases NEIL1 and NEIL3

Irina G. Minko[a], **Plamen P. Christov**[b], **Liang Li**[c], **Michael P. Stone**[c], **Amanda K. McCullough**[a,d], and **R. Stephen Lloyd**[a,d,e,*]

[a]Oregon Institute of Occupational Health Sciences, Oregon Health & Science University, Portland, OR 97239, United States

[b]Vanderbilt Institute of Chemical Biology, Vanderbilt University School of Medicine, Vanderbilt University, Nashville, TN 37235, United States

[c]Department of Chemistry and Biochemistry, Vanderbilt-Ingram Cancer Center, Vanderbilt Institute of Chemical Biology, Vanderbilt University, Nashville, TN 37235, United States

[d]Department of Molecular and Medical Genetics, Oregon Health & Science University, Portland, OR 97239, United States

[e]Department of Physiology and Pharmacology, Oregon Health & Science University, Portland, OR 97239, United States

Abstract

A variety of agents cause DNA base alkylation damage, including the known hepatocarcinogen aflatoxin B_1 (AFB_1) and chemotherapeutic drugs derived from nitrogen mustard (NM). The N7 site of guanine is the primary site of alkylation, with some N7-deoxyguanosine adducts undergoing imidazole ring-opening to stable mutagenic N^5-alkyl formamidopyrimidine (Fapy-dG) adducts. These adducts exist as a mixture of canonical β- and unnatural α-anomeric forms. The β species are predominant in double-stranded (ds) DNA. Recently, we have demonstrated that the DNA glycosylase NEIL1 can initiate repair of AFB_1-Fapy-dG adducts both *in vitro* and *in vivo,* with *Neil1*$^{-/-}$ mice showing an increased susceptibility to AFB_1-induced hepatocellular carcinoma.

Here, we hypothesized that NEIL1 could excise NM-Fapy-dG and that NEIL3, a closely related DNA glycosylase, could excise both NM-Fapy-dG and AFB_1-Fapy-dG. Product formation from the reaction of human NEIL1 with ds oligodeoxynucleotides containing a unique NM-Fapy-dG followed a bi-component exponential function under single turnover conditions. Thus, two adduct conformations were differentially recognized by hNEIL1. The excision rate of the major form (~ 13.0 min^{-1}), presumed to be the β-anomer, was significantly higher than that previously reported for 5-hydroxycytosine, 5-hydroxyuracil, thymine glycol (Tg), and AFB_1-Fapy-dG. Product generation from the minor form was much slower (~ 0.4 min^{-1}), likely reflecting the rate of

*Corresponding author at: Oregon Institute of Occupational Health Sciences, Oregon Health & Science University, Portland, OR 97239, United States.lloydst@ohsu.edu (R.S. Lloyd).

Conflict of interest

None declared.

conversion of the α anomer into the β anomer. *Mus musculus* NEIL3 (MmuNEIL3Δ324) excised NM-Fapy-dG from single-stranded (ss) DNA (turnover rate of ~0.4 min^{-1}), but not from ds DNA. Product formation from ss substrate was incomplete, presumably because of a substantial presence of the α anomer. *Mmu*NEIL3Δ324 could not initiate repair of AFB_1-Fapy-dG in either ds or ss DNA. Overall, the data suggest that both NEIL1 and NEIL3 may protect cells against cytotoxic and mutagenic effects of NM-Fapy-dG, but NEIL1 may have a unique role in initiation of base excision repair of AFB_1-Fapy-dG.

Keywords

Base excision repair; Ring-fragmented purines; DNA alkylation; Aflatoxin; Nitrogen mustard

1. Introduction

Cellular DNA is susceptible to attack by alkylating agents that could originate from either normal metabolic processes or as result of exposure to various environmental toxicants. The latter compounds include aflatoxin B_1 (AFB_1), the product of *Aspergillus flavus* and related fungi that contaminate food crops. Chronic dietary exposure to AFB_1 represents an increased etiological risk for developing hepatocellular carcinoma (HCC) [1,2]. DNA alkylation is also induced by many chemotherapeutic drugs, such as temozolomide and nitrogen mustards (NMs), and is largely responsible for therapeutic effectiveness of these agents [3,4].

The guanine N7 atom is the most nucleophilic site within DNA bases [5] and is the primary target of alkylation (Fig. 1). Initial N7-deoxyguanosine (N7-dG) adducts can undergo secondary reactions because of the positive charge on the imidazole ring, yielding either an abasic site or the N^5-substituted formamidopyrimidine (Fapy-dG) adducts [6]. The alkyl-Fapy-dGs are more chemically stable than the corresponding N7-alkylated dGs, leading to much longer half-lives of the alkylated lesions in cellular DNA [6–9]. The analyses of DNA modifications in livers of Fischer rats that were intraperitoneally injected with a single AFB_1 dose demonstrated rapid disappearance of the original N7-dG adducts, with an apparent half-life of 7.5 h [8]. Approximately 20% of these adducts were converted to AFB_1-Fapy-dGs that became the dominant lesions in 24 h and persisted during the 72-h period studied. When DNA repair-proficient mice were intraperitoneally injected with a single, non-lethal AFB_1 dose, the AFB_1-N7-dG and AFB_1-Fapy-dG adducts were present in liver DNA 6 h post-injection at comparable levels, approximately 50 and 68 pmoles/mg, respectively [9]. By 48 h, the initial N7-dG adducts essentially disappeared, while the level of AFB_1-Fapy-dGs was reduced less than 2-fold. Although kinetics of conversion have not been addressed *in vivo* for the NM-induced adducts, N7-dG and Fapy-dG modifications were detected in cultured cancer cells treated for 24 h with bis(2-chloroethyl)amine at the levels of 970 and 180 adducts per 10^7 nucleotides, respectively [7]. As expected, this bifunctional agent also induced the formation of DNA crosslinks, including both NM-N7-dG-N7-dG (240 per 10^7 nucleotides) and NM-Fapy-dG-N7-dG (6 per 10^7 nucleotides).

Structural and biochemical investigations on Fapy-dG adducts are complicated by the fact that these adducts exist as a mixture of interconverting α- and β-anomeric forms (Fig. 1). The β species are predominant in double-stranded (ds) DNA. This has been shown for the temozolomide-induced methyl-Fapy-dG (Me-Fapy-dG) [10], NM-Fapy-dG [11], and AFB_1-Fapy-dG [12–15].

The N^5-substituted Fapy-dG adducts manifest a strong mutator phenotype. As demonstrated by analyses of sequence alterations following replication of site-specifically modified vectors in primate (simian kidney COS7) cells, the spectra of mutations induced by these lesions were dominated by base substitutions, with G to T transversions being most common [16–18]. The overall mutation frequencies measured for Me-Fapy-dG ranged from ~9 to 21%, depending on the local sequence context [16], and ~ 11–12% for NM-Fapy-dG [18]. The AFB_1-Fapy-dG adduct caused mutations at an unprecedentedly high ~97% frequency, including ~86% G to T transversions [17]. This spectrum parallels the mutational signature of AFB_1 that was determined using DNA from exposed cultured cells or experimental animals, or from AFB_1-associated HCCs [19–23].

AFB_1-Fapy-dG has been long recognized as a substrate for nucleotide excision repair [24,25]. However, we recently demonstrated that this lesion is removed by base excision repair. We showed that DNA glycosylase NEIL1, a member of the Fpg/Nei glycosylase family, could excise AFB_1-Fapy-dG from site-specifically modified oligodeoxynucleotides *in vitro* and that *Neil1*$^{-/-}$ mice accumulated significantly more of these lesions in liver DNA following a single AFB_1 injection than *Neil1* $^{+/+}$ mice. Furthermore, *Neil1* $^{-/-}$ mice showed an increased susceptibility to AFB_1-induced HCC versus control mice, implicating the AFB_1-Fapy-dG adduct as a major contributor to AFB_1-induced carcinogenesis [9].

In addition to AFB_1-Fapy-dG, NEIL1 recognizes unsubstituted Fapy-dG and Fapy-dA, Me-Fapy-dG, thymine glycol (Tg), psoralen-induced adducts, and oxidation products of 8-oxo-deoxyguanosine, guanidino-hydantoin and spiroiminohydantoin (Sp) [26–37]. NEIL3, another member of the Fpg/Nei DNA glycosylase family, recognizes a broad class of lesions that significantly overlaps with that of NEIL1 [37–42]. Germane to the present study, the shared substrates include unsubstituted Fapy-dG and Me-Fapy-dG. Thus, we hypothesized that NEIL3 would recognize AFB1-Fapy-dG and that both NEIL1 and NEIL3 would be able to initiate repair of NM-Fapy-dG. To address these possibilities, we measured the kinetics of product formation for the reaction of site-specifically modified oligodeoxynucleotides containing these or control lesions with human NEIL1 (hNEIL1) [32] or a truncated form of *Mus musculus* NEIL3 (*Mmu*NEIL3Δ324) [38,42].

2. Materials and methods

2.1. DNA substrates

The oligodeoxynucleotides containing Me-Fapy-dG, NM-Fapy-dG, or AFB_1-Fapy-dG were synthesized as previously described [10,11,43]. The non-adducted and Tg-containing oligodeoxynucleotides were obtained from Integrated DNA Technologies, Inc. The sequences of modified DNAs were 5′-ACCACGCTAGCXAGTCCTAACAAC-3′ (where X is Me-Fapy-dG or NM-Fapy-dG) or 5′-ACCACTACTATXATTCATAACAAC-3′ (where X

is AFB_1-Fapy-dG or Tg). The adducted oligodeoxynucleotides were labeled at the 5′ termini using [γ–^{32}P]ATP (PerkinElmer Life Sciences) and T4 polynucleotide kinase (New England BioLabs). The ds substrates were prepared as described in our prior study [9].

2.2. Enzymes

The hNEIL1 and *Mmu*NEIL3Δ324 glycosylases were purified as described in Roy et al. [32] and Liu et al. [42], respectively. *Mmu*NEIL3Δ324 was the generous gift of Dr. Sylvie Doublié (University of Vermont). Human apurinic/apyrimidinic (AP) endonuclease, APE1, was purchased from New England BioLabs Inc.

2.3. DNA glycosylase assays

The glycosylase reactions were conducted at 37 °C in buffers previously optimized and used for hNEIL1 (20 mM Tris-HCl, pH 7.4, 100 mM KCl, and 100 μg/ml BSA) [9,32] or *Mmu*NEIL3Δ324 (20 mM HEPES-Na, pH 7.0, 50 mM NaCl, 100 μg/ml BSA, 0.01% Triton X-100, and 1 mM dithiothreitol) [38,42]. In order to analyze glycosylase activity independently of the AP lyase activity, the reactions were terminated by addition of equal volume of 0.5 N NaOH, followed by incubation at 90 °C for 5 min. Enzyme concentrations, substrate concentrations, and incubation times varied and are specified in the figures or figure legends. The rate constants were measured under single turnover conditions as previously described [9]. Following separation by polyacrylamide gel electrophoresis, the reaction products were visualized using a Personal Molecular Imager™ System (Bio-Rad). The product was quantified from a phosphor screen image by the Quantity One Software (Bio-Rad). The percent of non-specific products, amplitude of reaction, and rate constants were calculated using Kalei-daGraph software. All experiments were repeated at least three times, with representative gel images and curves shown. The data were expressed as average ± standard deviation.

3. Results and discussion

3.1. hNEIL1 can initiate repair of NM-Fapy-dG

A site-specifically modified ds oligodeoxynucleotide (24-mer) containing a NM-Fapy-dG at the 12th position opposite deoxycytidine was used to examine hNEIL1 ability to initiate repair of NM-Fapy-dG; the same construct, except with a Tg adduct opposite deoxyadenosine was used as a control. Since the release of NEIL1 from its products is rate limiting, the reactions were conducted under single turnover conditions. The kinetics of product formation for the control Tg substrate followed a single exponential rise (Eq. (1)), with a strong correlation between the experimental points and the curve ($R^2 > 0.99$), (Fig. 2A & C). The observed excision rate constant (k_{obs}) calculated from this fit was 1.2 min^{-1}, which was in good agreement with results of our prior study (1.4 min^{-1}) [9] and the observed rate constant reported for Tg by Krishnamurthy and colleagues (1.3 min^{-1}) [34].

The experimental points from the same analysis of the NM-Fapy-dG-containing DNA significantly deviated from a single exponential rise curve, but fitted with strong correlation ($R^2 > 0.99$) to a bi-component exponential rise function (Eq. (2)) (Fig. 2B & C). We calculated rate constants of 13.0 ± 6.4 min^{-1} (k_{obs1}) and 0.4 ± 0.2 min^{-1} (k_{obs2}) from three

independent experiments; the corresponding extrapolated amplitudes were 43.0 ± 13.0% (S_1) and 36.0 ± 1.0% (S2) of the initial substrate. The non-specific cleavage product accounted for 12.5 ± 2.0%.

To address the nature of non-specific cleavage, DNA was incubated in the absence of enzyme, with or without subsequent treatment with NaOH. In addition, DNA was reacted with APE1. These tests demonstrated that DNA was stable under the glycosylase reaction conditions, and that preexisting nicks and abasic sites accounted for only a small fraction of non-specific product (< 3% of the initial DNA); the non-specific cleavage largely occurred during alkali treatment (data not shown).

The DNA substrate existing as two or more structures that were differentially recognized by hNEIL1 could explain the complex kinetics of product formation described above. In support of this explanation, NM-Fapy-dG is known to exist as a slowly equilibrating mixture of α- and β-anomeric forms (Fig. 1), with the β form being predominant in ds DNA [11]. In addition, various configurations of the modified base are possible based on analogy with Me-Fapy-dG [44] and AFB_1-Fapy-dG [12–15], including geometrical isomers of the formamide and atropisomers at the C5-N^5 bond. Since the β anomer is a natural state of nucleosides in DNA, we inferred that hNEIL1 incised β-anomeric adducts more efficiently. This interpretation would be consistent with our prior finding that only the β anomer of AFB_1-Fapy-dG is a substrate for hNEIL1 [9].

We considered several possibilities concerning the slower reacting fraction. In particular, hNEIL1 could discriminate between different base configurations of β-NM-Fapy-dG (e.g., formamide geometric isomers or atropisomers), as was previously observed for diastereomers of Sp [34]. Structural data regarding the isomeric composition of NM-Fapy-dG in ds DNA that would either support or dispute this hypothesis are currently unavailable. However, the ratio of differentially processed species, as estimated from the extrapolated amplitudes, was ~ 1.2 to 1, with the dominating species being a preferred NEIL1 substrate. Since this ratio is close to the previously estimated β/α anomeric composition of NM-Fapy-dG in ds DNA [11], we hypothesize that the products formed in the slower reaction originated from the α form. The probability of hNEIL1 directly acting on the α form is low, as a major rearrangement of DNA substrate would be required for proper positioning of the glycosidic bond in the active site. Thus, we favor the hypothesis that product formation through this route was the result of slow, rate-limiting conversion of the α anomer into the β anomer, followed by fast incision at the β anomer. This scenario requires that the enzyme environment accelerates the rate of interconversion between two anomers, since the equilibration of anomers in free ds DNA occurs over a period of days [11].

Interestingly, product formation of the AFB_1-Fapy-dG followed a single exponential rise under identical conditions (Eq. (1)) [9]. A likely reason for this result is that AFB_1-Fapy-dG exists in ds DNA almost exclusively in the β anomeric form [12–15]. The stabilization of the overall structure has been attributed to the stacking interactions of the AFB_1 moiety with the 5′ neighboring base. Since the NM moiety is expected to be more solvent exposed, the observed heterogeneity of this adduct can be easily explained. Thus, collectively with our

prior analyses on hNEIL1-catalyzed excision of AFB_1-Fapy-dG [9], the present data on NM-Fapy-dG provide further evidence for structural differences between these two adducts.

The observed rate constant of hNEIL1-catalyzed excision of β-NM-Fapy-dG (13.0 ± 6.4 min^{-1}) was ~ 75-fold higher than that estimated for p-AFB_1-Fapy-dG (0.17 ± 0.03 min^{-1}) [9], which can be attributed to both size and structural differences, especially in regard to intercalation as discussed above. The excision rate of β-NM-Fapy-dG by hNEIL1 was much faster than the excision rates of 5-hydroxycytosine (0.24 min^{-1}), 5-hydroxyuracil (0.14 min^{-1}), and Tg (1.2–1.4 min^{-1}), but significantly slower than that of guanidinohydantoin (104 min^{-1}), Sp1 (117 min^{-1}), and Sp2 (139 min^{-1}) in their respective canonical base pairs [9,34,36]. Further analyses are needed to compare NM-Fapy-dG and the unsubstituted Fapy-dG regarding both the incision rates and kinetics.

3.2. MmuNEIL3Δ324 can initiate repair of NM-Fapy-dG but notAFB_1-Fapy-dG

Human and mouse NEIL3 orthologs share 74% sequence identity.

Prior analyses have demonstrated that hNEIL3Δ324 and MmuNEIL3A324 exhibit similar activity on a number of DNA substrates, including Tg and Sp [42]. The direct comparison of *Mmu*NEIL3Δ324 with *Mmu*NEIL3 showed that the preferred substrates, such as Sp, guanidinohydantoin, Me-Fapy-dG, and an abasic site in single-stranded (ss) DNA, were recognized by these enzymes equally well [38]. Thus, we utilized *Mmu*NEIL3Δ324 as a model for characterization of NEIL3 glycosylase activity.

An initial assessment for the ability of *Mmu*NEIL3Δ324 to initiate repair of NM- and AFB_1-induced Fapy-dG lesions was performed with ds oligodeoxynucleotides using a 100:1 ratio of enzyme to substrate (Fig. 3A). DNA substrates were constructed as above and included NM-Fapy-dG, AFB_1-Fapy-dG, and two reference adducts, Me-Fapy-dG and Tg. In control reactions with NEIL1, all four substrates were cleaved to near completion (Fig. 3A). In agreement with previous results [38], recognition of Me-Fapy-dG and Tg by *Mmu*NEIL3Δ324 in the context of ds DNAs was poor, with only 4.0 ± 1.1 and 3.5 ± 1.1% product formed, respectively. No evidence was found for *Mmu*NEIL3Δ324-catalyzed excision of either NM-Fapy-dG or AFB_1-Fapy-dG from ds DNA.

NEIL3 prefers ss DNA [38–42]. Thus, the *Mmu*NEIL3Δ324-initiated repair of substituted Fapy-dG adducts was examined using the same set of modified oligodeoxynucleotides but in ss form (Fig. 3B). These data demonstrated that *Mmu*NEIL3Δ324 recognized NM-Fapy-dG and Me-Fapy-dG equally and both were better substrates than Tg. When the product accumulation was not limited by substrate availabilities, at a 1:1 enzyme to DNA ratio, the amount of products, corrected for nonspecific cleavage, was 19.3 ± 2.6, 22.4 ± 4.0, and 4.1 ± 0.8%, respectively. A similar trend was also observed at 10-fold excess of *Mmu*NEIL3Δ324, with 36.0 ± 1.6, 35.5 ± 2.7, and 22.2 ± 1.3% product formation, respectively. In contrast, no incision was detected at these enzyme concentrations on AFB_1-Fapy-dG-containing ss DNA. We reexamined the ability of *Mmu*NEIL3Δ324 to initiate repair of AFB_1-Fapy-dG in ss DNA using 100-fold excess enzyme concentration over substrate concentration but observed no products (data not shown).

To further elucidate the *Mmu*NEIL3Δ324-catalyzed repair of NM-Fapy-dG from ss DNA, reactions were conducted under single turnover conditions (Fig. 3C). The kinetics of product accumulation strongly correlated with a single exponential rise function (Eq. [1], $R^2 > 0.99$). The observed rate constant (k_{obs}) was 0.4 ± 0.1 min^{-1} and the extrapolated amplitude (S) was 33.5 ± 2.0% of the initial substrate. We assume that these values reflect the excision rate constant of *Mmu*NEIL3Δ324 for the β-anomeric adduct and the fraction of these species in ss DNA, respectively. Consistent with this interpretation, the β anomer was estimated to constitute ~ 35–40% NM-Fapy-dG when the lesion was positioned at the primer/template junction on template DNA [18]. The extrapolated non-specific cleavage product accounted for 19.0 ± 1.0%, which was notably higher relative to that observed in hNEIL1-catalyzed reactions using ds DNA (12.5 ± 2.0%). The latter difference probably reflects a decreased stability of NM-Fapy-dG in ss versus ds DNA, likely because of a higher fraction of the α-anomeric form.

Relative to Sp1, which is an excellent substrate for *Mmu*NEIL3Δ324, the rate of excision of β-NM-Fapy-dG in ss DNA was slow. The k_{obs} values reported for Sp1 in ss and ds DNA were ~184 and 3.2 min^{-1}, respectively [38]. However, excision of NM-Fapy-dG from ss DNA under multiple turnover conditions (Fig. 3B) was more efficient than that of Tg and comparable with the excision of Me-Fapy-dG.

In conclusion, our study has contributed to the characterization of substrate specificities of NEIL1 and NEIL3 and provides new insights into the conformation of the NM-Fapy-dG adduct. No evidence was found for the ability of *Mmu*NEIL3Δ324 to act on AFB_1-Fapy-dG, suggesting that the role of NEIL1 in base excision repair of this lesion could be unique. Consistent with the idea that there is no backup glycosylase to compensate for this NEIL1 function, *Neil1*$^{-/-}$ mice accumulated significantly more AFB_1-Fapy-dG adducts in liver DNA than *Neil1*$^{+/+}$ mice and showed an increased susceptibility to AFB_1-induced HCC [9].

The present study established that hNEIL1 and *Mmu*NEIL3Δ324 both could initiate repair of NM-Fapy-dG. Except for the oxidation products of 8-oxo-deoxyguanosine, NM-Fapy-dG was excised as well as other, previously known substrates of these glycosylases, or better. Thus, NEIL1 and NEIL3 may protect cells against cytotoxic and mutagenic effects of NM-Fapy-dG. The kinetics of NM-Fapy-dG excision showed that the adduct existed as a complex mixture of species that are differentially recognized by hNEIL1 and *Mmu*NEIL3Δ324. We infer that only the β-anomeric form of the adduct is a substrate for these glycosylases. The fraction of the incision-resistant α anomer was substantial in both ss and ds DNA. The contribution of individual anomers to biological effects of DNA adducts is an important but poorly elucidated problem. Specifically with regard to the NM-Fapy-dG adduct, we recently demonstrated that although the α anomer could contribute to induction of base substitutions during replication of ss vector DNA in primate cells, it was a significantly stronger block for DNA synthesis than its β counterpart [18]. Thus, the α anomer is anticipated to be more cytotoxic and in the context of genomic DNA, is hypothesized to cause gross DNA alterations rather than point mutations. In addition, our study demonstrated that kinetic analyses conducted under single turnover conditions can be informative regarding the anomeric composition of Fapy-dG adducts in DNA. Using hNEIL1 and *Mmu*NEIL3Δ324 for evaluation of the anomeric ratio in ds and ss DNA, effects

of the sequence context, substituent nature, and other parameters on this ratio can be addressed.

Acknowledgments

We thank Dr. Sylvie Doublié (University of Vermont) for the kind gift of *Mmu*NEIL3Δ324 and Dr. Carmelo Rizzo (Vanderbilt University) for insightful discussions and editing.

This work was supported by the National Institutes of Health Grants P01 CA160032, P30 CA068485, R01 CA055678, and R01 ES029357.

Abbreviations:

AFB_1	aflatoxin B_1
NM	nitrogen mustard
N7-dG	N7-substituted deoxyguanosine
Fapy-dG	formamidopyrimidine deoxyguanosine adduct
ds	double-stranded
ss	single-stranded
HCC	hepatocellular carcinoma
Me	methyl
Tg	thymine glycol
Sp	spiroiminohydantoin
AP	apurinic/apyrimidinic

References

[1]. Blonski W, Kotlyar DS, Forde KA, Non-viral causes of hepatocellular carcinoma, World J. Gastroenterol. 16 (2010) 3603–3615. [PubMed: 20677332]

[2]. Klungboonkrong V, Das D, McLennan G, Molecular mechanisms and targets of therapy for hepatocellular carcinoma, J. Vasc. Interv. Radiol. 28 (2017) 949–955, 10.1016/j.jvir.2017.03.002. [PubMed: 28416267]

[3]. Erasimus H, Gobin M, Niclou S, Van Dyck E, DNA repair mechanisms and their clinical impact in glioblastoma, Res. Rev. Res. 769 (2016) 19–35, 10.1016/j.mrrev.2016.05.005.

[4]. Singh RK, Kumar S, Prasad DN, Bhardwaj TR, Therapeutic journery of nitrogen mustard as alkylating anticancer agents: historic to future perspectives, Eur. J. Med. Chem. 151 (2018) 401–433, 10.1016/j.ejmech.2018.04.001. [PubMed: 29649739]

[5]. Pullman A, Pullman B, Molecular electrostatic potential of the nucleic acids, Q. Rev. Biophys. 14 (1981) 289–380. [PubMed: 7027300]

[6]. Gates KS, Nooner T, Dutta S, Biologically relevant chemical reactions of N7-alkylguanine residues in DNA, Chem. Res. Toxicol. 17 (2004) 839–856, 10.1021/tx049965c. [PubMed: 15257608]

[7]. Gruppi F, Hejazi L, Christov PP, Krishnamachari S, Turesky RJ, Rizzo CJ, Characterization of nitrogen mustard formamidopyrimidine adduct formation of bis (2-chloroethyl)ethylamine with

calf thymus DNA and a human mammary cancer cell line, Chem. Res. Toxicol. 28 (2015) 1850–1860, 10.1021/acs.chemrestox.5b00297. [PubMed: 26285869]

[8]. Croy RG, Wogan GN, Temporal patterns of covalent DNA adducts in rat liver after single and multiple doses of aflatoxin B1, Cancer Res. 41 (1981) 197–203. [PubMed: 7448760]

[9]. Vartanian V, Minko IG, Chawanthayatham S, Egner PA, Lin YC, Earley LF, Makar R, Eng JR, Camp MT, Li L, Stone MP, Lasarev MR, Groopman JD, Croy RG, Essigmann JM, McCullough AK, Lloyd RS, NEIL1 protects against aflatoxin-induced hepatocellular carcinoma in mice, Proc. Natl. Acad. Sci. U. S. A. 114 (2017) 4207–4212, 10.1073/pnas.1620932114. [PubMed: 28373545]

[10]. Christov PP, Banerjee S, Stone MP, Rizzo CJ, Selective incision of the α-N5-methyl-formamidopyrimidine anomer by Escherichia coli endonuclease IV, J. Nucleic Acids (2010), https://doi.org/10.406½010/850234.

[11]. Christov PP, Son KJ, Rizzo CJ, Synthesis and characterization of oligonucleotides containing a nitrogen mustard formamidopyrimidine monoadduct of deoxyguanosine, Chem. Res. Toxicol. 27 (2014) 1610–1618, 10.1021/tx5002354. [PubMed: 25136769]

[12]. Mao H, Deng Z, Wang F, Harris TM, Stone MP, An intercalated and thermally stable FAPY adduct of aflatoxin B1 in a DNA duplex: structural refinement from 1H NMR, Biochemistry 37 (1998) 4374–4387, 10.1021/bi9718292. [PubMed: 9521757]

[13]. Brown KL, Deng JZ, Iyer RS, Iyer LG, Voehler MW, Stone MP, Harris CM, Harris TM, Unraveling the aflatoxin-FAPY conundrum: structural basis for differential replicative processing of isomeric forms of the formamidopyrimidine-type DNA adduct of aflatoxin B1, J. Am. Chem. Soc. 128 (2006) 15188–15199, 10.1021/ja063781y. [PubMed: 17117870]

[14]. Brown KL, Voehler MW, Magee SM, Harris CM, Harris TM, Stone MP, Structural perturbations induced by the a-anomer of the aflatoxin B1 for-mamidopyrimidine adduct in duplex and single-strand DNA, J. Am. Chem. Soc. 131 (2009) 16096–16107, 10.1021/ja902052v. [PubMed: 19831353]

[15]. Li L, Brown KL, Ma R, Stone MP, DNA sequence modulates geometrical isomerism of the trans-8,9-dihydro-8-(2,6-diamino-4-oxo-3,4-dihydropyrimid-5-yl-formamido)-9-hydroxy aflatoxin B1 adduct, Chem. Res. Toxicol. 28 (2015) 225–237, 10.1021/tx5003832. [PubMed: 25587868]

[16]. Earley LF, Minko IG, Christov PP, Rizzo CJ, Lloyd RS, Mutagenic spectra arising from replication bypass of the 2,6-diamino-4-hydroxy-N5-methyl for-mamidopyrimidine adduct in primate cells, Chem. Res. Toxicol. 26 (2013) 1108–1114, 10.1021/tx4001495. [PubMed: 23763662]

[17]. Lin YC, Li L, Makarova AV, Burgers PM, Stone MP, Lloyd RS, Molecular basis of aflatoxin-induced mutagenesis-role of the aflatoxin B1-formamidopyrimidine adduct, Carcinogenesis 35 (2014) 1461–1468, 10.1093/carcin/bgu003. [PubMed: 24398669]

[18]. Minko IG, Rizzo CJ, Lloyd RS, Mutagenic potential of nitrogen mustard-induced formamidopyrimidine DNA adduct: contribution of the non-canonical α -anomer, J. Biol. Chem. 292 (2017) 18790–18799, 10.1074/jbc.M117.802520. [PubMed: 28972137]

[19]. Bressac B, Kew M, Wands J, Ozturk M, Selective G to T mutations of p53 gene in hepatocellular carcinoma from southern Africa, Nature 350 (1991) 429–431, 10.1038/350429a0. [PubMed: 1672732]

[20]. Hsu IC, Metcalf RA, Sun T, Welsh JA, Wang NJ, Harris CC, Mutational hotspot in the p53 gene in human hepatocellular carcinomas, Nature 350 (1991) 427–428, 10.1038/350427a0. [PubMed: 1849234]

[21]. Chawanthayatham S, Valentine CC 3rd, Fedeles BI, Fox EJ, Loeb LA, Levine SS, Slocum SL, Wogan GN, Croy RG, Essigmann JM, Mutational spectra of aflatoxin B1 in vivo establish biomarkers of exposure for human hepatocellular carcinoma, Proc. Natl. Acad. Sci. U. S. A. 114 (2017) E3101–E3109, 10.1073/pnas.1700759114. [PubMed: 28351974]

[22]. Huang MN, Yu W, Teoh WW, Ardin M, Jusakul A, Ng AWT, Boot A, Abedi-Ardekani B, Villar S, Myint SS, Othman R, Poon SL, Heguy A, Olivier M, Hollstein M, Tan P, Teh BT, Sabapathy K, Zavadil J, Rozen SG, Genome-scale mutational signatures of aflatoxin in cells, mice, and human tumors, Genome Res. 27 (2017) 1475–1486, 10.1101/gr.220038.116. [PubMed: 28739859]

[23]. Zhang W, He H, Zang M, Wu Q, Zhao H, Lu LL, Ma P, Zheng H, Wang N, Zhang Y, He S, Chen X, Wu Z, Wang X, Cai J, Liu Z, Sun Z, Zeng YX, Qu C, Jiao Y, Genetic features of aflatoxin-associated hepatocellular carcinoma, Gastroenterology 153 (2017) 249–262, 10.1053/j.gastro.2017.03024e242. [PubMed: 28363643]

[24]. Alekseyev YO, Hamm ML, Essigmann JM, Aflatoxin B1 formamidopyrimidine adducts are preferentially repaired by the nucleotide excision repair pathway in vivo, Carcinogenesis 25 (2004) 1045–1051, 10.1093/carcin/bgh098. [PubMed: 14742311]

[25]. Leadon SA, Tyrrell RM, Cerutti PA, Excision repair of aflatoxin B1-DNA adducts inhuman fibroblasts, Cancer Res. 41 (1981) 5125–5129. [PubMed: 6796265]

[26]. Hazra TK, Izumi T, Boldogh I, Imhoff B, Kow YW, Jaruga P, Dizdaroglu M, Mitra S, Identification and characterization of a human DNA glycosylase for repair of modified bases in oxidatively damaged DNA, Proc. Natl. Acad. Sci. U. S. A. 99 (2002) 3523–3528, 10.1073/pnas.062053799. [PubMed: 11904416]

[27]. Bandaru V, Sunkara S, Wallace SS, Bond JP, A novel human DNA glycosylase that removes oxidative DNA damage and is homologous to Escherichia coli endonuclease VIII, DNA Repair (Amst.) 1 (2002) 517–529. [PubMed: 12509226]

[28]. Morland I, Rolseth V, Luna L, Rognes T, Bjoras M, Seeberg E, Human DNA glycosylases of the bacterial Fpg/MutM superfamily: an alternative pathway for the repair of 8-oxoguanine and other oxidation products in DNA, Nucleic Acids Res. 30 (2002) 4926–4936. [PubMed: 12433996]

[29]. Takao M, Kanno S, Kobayashi K, Zhang QM, Yonei S, van der Horst GT, Yasui A, A back-up glycosylase in Nth1 knock-out mice is a functional Nei (endonuclease VIII) homologue, J. Biol. Chem. 277 (2002) 42205–42213, 10.1074/jbc.M206884200. [PubMed: 12200441]

[30]. Rosenquist TA, Zaika E, Fernandes AS, Zharkov DO, Miller H, Grollman AP, The novel DNA glycosylase, NEIL1, protects mammalian cells from radiation-mediated cell death, DNA Repair (Amst.) 2 (2003) 581–591. [PubMed: 12713815]

[31]. Jaruga P, Birincioglu M, Rosenquist TA, Dizdaroglu M, Mouse NEIL1 protein is specific for excision of 2,6-diamino-4-hydroxy-5-formamidopyrimidine and 4,6-diamino-5-formamidopyrimidine from oxidatively damaged DNA, Biochemistry 43 (2004) 15909–15914, 10.1021/bi048162l. [PubMed: 15595846]

[32]. Roy LM, Jaruga P, Wood TG, McCullough AK, Dizdaroglu M, Lloyd RS, Human polymorphic variants of the NEIL1 DNA glycosylase, J. Biol. Chem. 282 (2007) 15790–15798, 10.1074/jbc.M610626200. [PubMed: 17389588]

[33]. Couve-Privat S, Mace G, Rosselli F, Saparbaev MK, Psoralen-induced DNA adducts are substrates for the base excision repair pathway in human cells, Nucleic Acids Res. 35 (2007) 5672–5682, 10.1093/nar/gkm592. [PubMed: 17715144]

[34]. Krishnamurthy N, Zhao X, Burrows CJ, David SS, Superior removal ofhydantoin lesions relative to other oxidized bases by the human DNA glycosylase hNEIL1, Biochemistry 47 (2008) 7137–7146, 10.1021/bi800160s. [PubMed: 18543945]

[35]. Prakash A, Carroll BL, Sweasy JB, Wallace SS, Doublie S, Genome and cancer single nucleotide polymorphisms of the human NEIL1 DNA glycosylase: activity, structure, and the effect of editing, DNA Repair (Amst.) 14 (2014) 17–26, 10.1016/j.dnarep.2013.12.003. [PubMed: 24382305]

[36]. Vik ES, Alseth I, Forsbring M, Helle IH, Morland I, Luna L, Bjoras M, Dalhus B, Biochemical mapping of human NEIL1 DNA glycosylase and AP lyase activities, DNA Repair (Amst.) 11 (2012) 766–773, 10.1016/j.dnarep.201207.002. [PubMed: 22858590]

[37]. Martin PR, Couve S, Zutterling C, Albelazi MS, Groisman R, Matkarimov BT, Parsons JL, Elder RH, Saparbaev MK, The human DNA glycosylases NEIL1 and NEIL3 excise psoralen-induced DNA-DNA cross-links in a four-stranded DNA structure, Sci. Rep. 7 (2017) 17438, 10.1038/s41598-017-17693-4. [PubMed: 29234069]

[38]. Liu M, Bandaru V, Bond JP, Jaruga P, Zhao X, Christov PP, Burrows CJ, Rizzo CJ, Dizdaroglu M, Wallace SS, The mouse ortholog of NEIL3 is a functional DNA glycosylase in vitro and in vivo, Proc. Natl. Acad. Sci. U. S. A. 107 (2010) 4925–4930, 10.1073/pnas.0908307107. [PubMed: 20185759]

[39]. Liu M, Doublie S, Wallace SS, Neil3, the final frontier for the DNA glycosylases that recognize oxidative damage, Mutat. Res. 743–744 (2013) 4–11, 10.1016/j.mrfmmm.2012.12.003.

[40]. Liu M, Imamura K, Averill AM, Wallace SS, Doublie S, Structural characterization of a mouse ortholog of human NEIL3 with a marked preference for singlestranded DNA, Structure 21 (2013) 247–256, 10.1016/j.str.2012.12.008. [PubMed: 23313161]

[41]. Krokeide SZ, Laerdahl JK, Salah M, Luna L, Cederkvist FH, Fleming AM, Burrows CJ, Dalhus B, Bjoras M, Human NEIL3 is mainly a monofunctional DNA glycosylase removing spiroimindiohydantoin and guanidinohydantoin, DNA Repair (Amst.) 12 (2013) 1159–1164, 10.1016/j.dnarep.2013.04.026. [PubMed: 23755964]

[42]. Liu M, Bandaru V, Holmes A, Averill AM, Cannan W, Wallace SS, Expression and purification of active mouse and human NEIL3 proteins, Protein Expr. Purif. 84 (2012) 130–139, 10.1016/j.pep.2012.04.022. [PubMed: 22569481]

[43]. Banerjee S, Brown KL, Egli M, Stone MP, Bypass of aflatoxin B1 adducts by the Sulfolobus solfataricus DNA polymerase IV, J. Am. Chem. Soc. 133 (2011) 12556–12568, 10.1021/ja2015668. [PubMed: 21790157]

[44]. Bamberger SN, Malik CK, Voehler MW, Brown SK, Pan H, Johnson-Salyard TL, Rizzo CJ, Stone MP, Configurational and conformational equilibria of N6-(2-Deoxy-D-erythro-pentofuranosyl)-2,6-diamino-3,4-dihydro-4-oxo-5-N-methylformamidopyrimidine (MeFapy-dG) lesion in DNA, Chem. Res. Toxicol. 31 (2018) 924–935, 10.1021/acs.chemrestox.8b00135. [PubMed: 30169026]

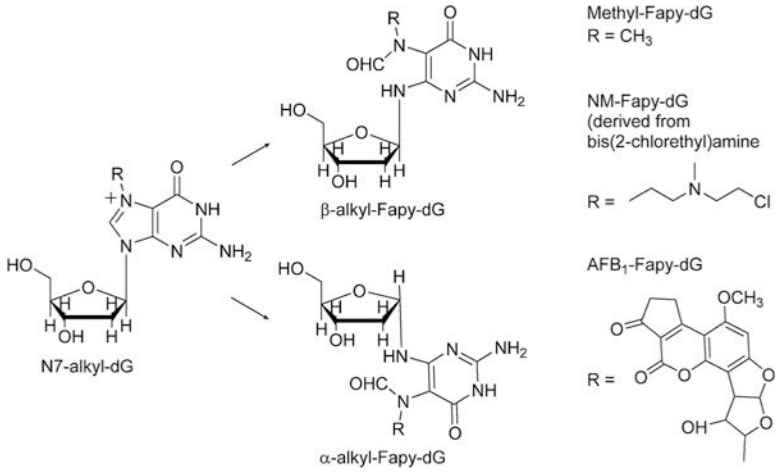

Fig. 1.

Formation of N^6-substituted formamidopyrimidine-dG adducts.

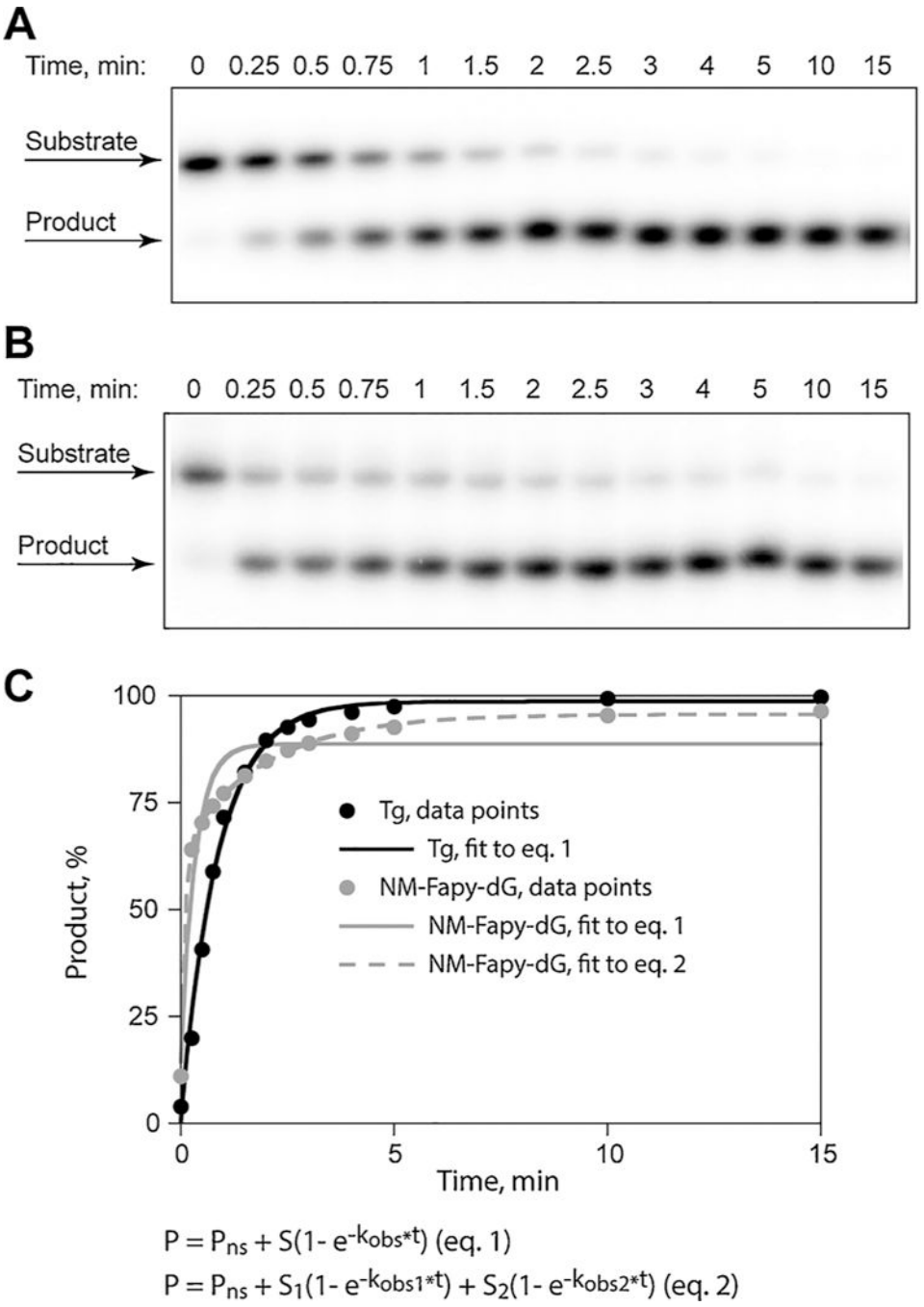

Fig. 2.

hNEILl-catalyzed incision at NM-Fapy-dG. The reactions were conducted at 37 °C in the presence of hNEIL1 (750 nM) using ^{32}P-labeled ds oligodeoxynucleotides (20 nM) that contained either Tg (A) or NM-Fapy-dG (B). Aliquots were removed at the indicated times, and following separation by gelelectrophoresis, DNA was visualized using a phosphor screen and a Personal Molecular Imager™ System (Bio-Rad). Representative gel images are shown. The product formation (P) was plotted as a function of time (t) (C), and the nonspecific product (P_{ns}), amplitude of substrate used (S), and observed rate constant (k_{obs})

values were obtained from the best fit of the data to a single (Eq. (1)) or bi-component (Eq. (2)) exponential function using KaleidaGraph software.

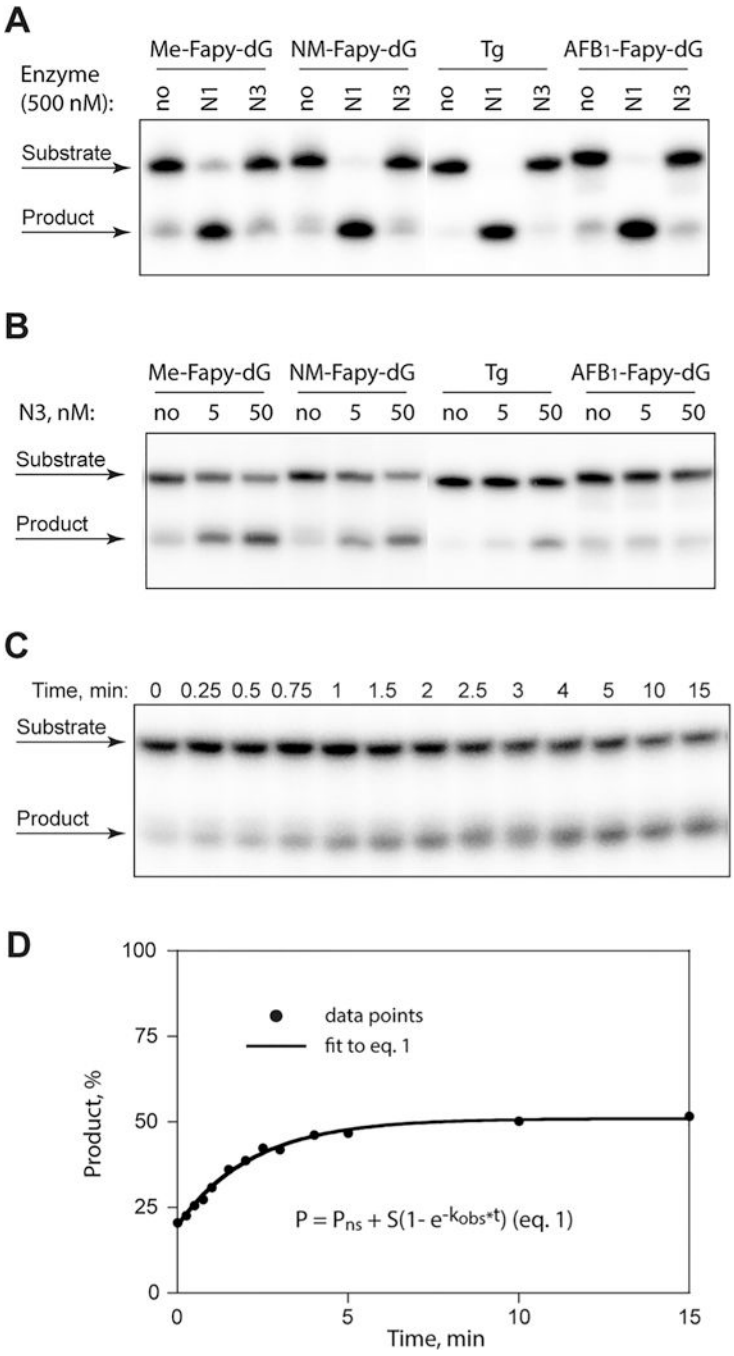

Fig. 3.

*Mmu*NEIL3Δ324-catalyzed incision at substituted Fapy-dG adducts. The reactions were conducted using ^{32}P-labeled ds (A) or ss (B) oligodeoxynucleotides (5 nM) for 30 min at 37 °C. The kinetic analysis (C, D) was performed at 37 °C in the presence of *Mmu*NEIL3Δ324 (750 nM) using ^{32}P-labeled ss oligodeoxynucleotides (20 nM); aliquots were removed at the indicated times. Following separation by gelelectrophoresis, DNA was visualized using a phosphor screen and Personal Molecular Imager™ System (Bio-Rad). Representative gel images are shown (A–C). N1 and N3 denote hNEIL1 and

*Mmu*NEIL3Δ324, respectively. The product formation (P) was plotted as a function of time (t) (D), and the non-specific product (P_{ns}), amplitude of substrate used (S), and observed rate constant (k_{obs}) values were obtained from the best fit of the data to a single (Eq. (1)) exponential function using KaleidaGraph software.